Report
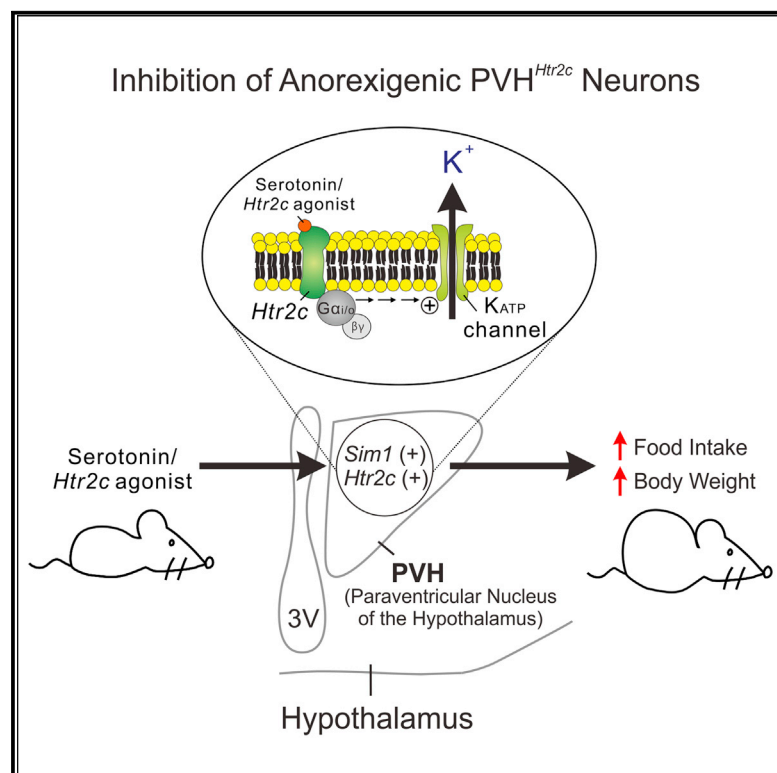
Gα_{i/o}-coupled *Htr2c* in the paraventricular nucleus of the hypothalamus antagonizes the anorectic effect of serotonin agents

Graphical abstract

Authors

Eun-Seon Yoo, Li Li, Lin Jia, ..., Yong Xu, Jong-Woo Sohn, Chen Liu

Correspondence

jwsohn@kaist.ac.kr (J.-W.S.),
chen.liu@utsouthwestern.edu (C.L.)

In brief

Yoo et al. show that *Htr2c*, the target of a former weight loss drug, can inhibit and promote food intake by coupling with distinct intracellular signaling events in different hypothalamic neurons. These findings may help explain the rather modest anti-obesity effects of *Htr2c* agonists.

Highlights

- Selective restoration *of Htr2c* in *Sim1* neurons promotes high-fat diet (HFD) feeding

- Selective deletion *of Htr2c* in *Sim1* neurons reduces HFD feeding

- PVH *Htr2c* neurons bidirectionally regulate food intake

- *Htr2c* is coupled to the Gα_{i/o}-K_{ATP} pathway in PVH neurons to inhibit their activity

CellPress

Report

Gα_{i/o}-coupled *Htr2c* in the paraventricular nucleus of the hypothalamus antagonizes the anorectic effect of serotonin agents

Eun-Seon Yoo,[1] Li Li,[2] Lin Jia,[2,6] Caleb C. Lord,[2] Charlotte E. Lee,[2] Shari G. Birnbaum,[4,5] Claudia R. Vianna,[2] Eric D. Berglund,[2] Kathryn A. Cunningham,[7] Yong Xu,[8,9] Jong-Woo Sohn,[1,*] and Chen Liu[2,3,5,10,*]

[1]Department of Biological Sciences, Korea Advanced Institute of Science and Technology, Daejeon 34141, Korea
[2]Center for Hypothalamic Research, Department of Internal Medicine, UT Southwestern Medical Center, Dallas, TX 75390, USA
[3]Department of Neuroscience, UT Southwestern Medical Center, Dallas, TX 75390, USA
[4]Department of Psychiatry, UT Southwestern Medical Center, Dallas, TX 75390, USA
[5]Peter O'Donnell Jr. Brain Institute, UT Southwestern Medical Center, Dallas, TX 75390, USA
[6]Department of Biological Sciences, The University of Texas at Dallas, Richardson, TX 75080, USA
[7]Center for Addiction Research and Department of Pharmacology and Toxicology, University of Texas Medical Branch, Galveston, TX 77555, USA
[8]Children's Nutrition Research Center, Department of Pediatrics, Baylor College of Medicine, Houston, TX 77030, USA
[9]Department of Molecular and Cellular Biology, Baylor College of Medicine, Houston, TX 77030, USA
[10]Lead contact
*Correspondence: jwsohn@kaist.ac.kr (J.-W.S.), chen.liu@utsouthwestern.edu (C.L.)
https://doi.org/10.1016/j.celrep.2021.109997

SUMMARY

The anorexigenic effect of serotonergic compounds has largely been attributed to activation of serotonin 2C receptors (*Htr2c*s). Using mouse genetic models in which *Htr2c* can be selectively deleted or restored (in *Htr2c*-null mice), we investigate the role of *Htr2c* in forebrain *Sim1* neurons. Unexpectedly, we find that *Htr2c* acts in these neurons to promote food intake and counteract the anorectic effect of serotonergic appetite suppressants. Furthermore, *Htr2c* marks a subset of *Sim1* neurons in the paraventricular nucleus of the hypothalamus (PVH). Chemogenetic activation of these neurons in adult mice suppresses hunger, whereas their silencing promotes feeding. In support of an orexigenic role of PVH *Htr2c*, whole-cell patch-clamp experiments demonstrate that activation of *Htr2c* inhibits PVH neurons. Intriguingly, this inhibition is due to Gα_{i/o}-dependent activation of ATP-sensitive K^+ conductance, a mechanism of action not identified previously in the mammalian nervous system.

INTRODUCTION

To combat the obesity epidemic as well as eating disorders such as anorexia nervosa, it is essential that we gain a better understanding of the complex regulation of feeding behaviors. Recent studies have identified several "feeding" neurons along the neuraxis where hunger and satiety cues are integrated with cognitive, emotional, and reward inputs (Kenny, 2011; Schwartz and Zeltser, 2013). These neuron populations may adopt different strategies to integrate neuronal and humoral signals and exert a positive or negative influence on food intake. For example, it has been shown that agouti-related protein (AgRP) neurons evoke voracious feeding behaviors through parallel and redundant forebrain feeding circuits, each of which is sufficient to drive food intake (Betley et al., 2013). On the other hand, multiple anorexigenic signals converge onto protein kinase C (PKC)-δ^+ neurons in the amygdala, supporting a model where diverse anorectic information is processed in one central node (Cai et al., 2014).

The brain serotonin (5-hydroxytryptamine or 5-HT) system is a key target for weight loss therapies. Pharmacological agents that

increase extracellular 5-HT content suppress food intake and reduce body weight (Wyler et al., 2017). The therapeutic potential of this pathway was highlighted by the demonstration that the anorexigenic actions of serotonergic agents such as d-fenfluramine (dFen, a key ingredient of the once-popular diet pill Fen/Phen) were mediated in part through the serotonin 2c receptor (*Htr2c*) (Tecott et al., 1995; Vickers et al., 1999). Subsequently, lorcaserin, an *Htr2c*-specific agonist, became one of the first US Food and Drug Administration (FDA)-approved weight loss drugs (Colman et al., 2012).

Htr2c is widely distributed in the brain, including in regions that are known to regulate food intake (Hoffman and Mezey, 1989). However, it is not clear whether the anorectic effects of 5-HT agents require coordinated actions of *Htr2c* at multiple feeding nodes or whether activation of *Htr2c* in discrete neuronal populations suppresses food intake in a parallel or convergent manner. We previously demonstrated that selective restoration of *Htr2c* only in pro-opiomelanocortin (POMC) neurons of *Htr2c*-null mice was sufficient to normalize body weight, food intake, and the anorectic responses to dFen (Xu et al., 2008).

Conversely, deletion of *Htr2c* specifically in these neurons during development or in adulthood resulted in hyperphagia and a blunted anorectic response to dFen (Berglund et al., 2013; D'Agostino et al., 2018). These findings identified POMC neurons as one of the sites where *Htr2c* regulates food intake.

In addition to POMC neurons, *Htr2c* is enriched in neurons of the paraventricular nucleus of the hypothalamus (PVH) that express the transcription factor single-minded 1 (*Sim1*) (Heisler et al., 2007). PVH *Sim1* neurons are physiologically relevant to regulation of feeding behaviors because haploinsufficiency of *Sim1* results in reduced numbers of PVH neurons and causes early-onset hyperphagia and obesity in rodents and humans (Holder et al., 2004; Michaud et al., 2001). Furthermore, deletion of methyl CpG binding protein 2 (Fyffe et al., 2008) or melanocortin 4 receptor (MC4R) specifically in *Sim1* neurons leads to hyperphagia and obesity in rodents (Li et al., 2021). Importantly, we demonstrated that the anorectic responses to 5-HT agents were blunted in mice heterozygous for *Sim1*, suggesting that *Sim1* neurons represent another important node in the brain to regulate such responses (Xu et al., 2010). In the current study, we investigated the role of *Htr2c* in feeding regulation in *Sim1* neurons using a combination of mouse genetic, chemogenetic, and electrophysiological analyses. Our studies led to the unexpected finding that *Htr2c* acts in *Sim1* neurons to promote food intake and counteract the anorexigenic actions of 5-HT agents. Moreover, although activation of *Htr2c* depolarizes anorexigenic POMC neurons in a phospholipase C (PLC)-dependent manner (Sohn et al., 2011), we find that its actions on PVH neurons are via the $G_{\alpha_{i/o}}$ pathway, resulting in hyperpolarization of PVH neurons.

RESULTS

Selective restoration of *Htr2c* only in *Sim1* neurons promotes food intake

We previously generated and characterized a re-activatable *Htr2c*-null mouse (*Htr2c^{nulll}*) in which transcription of endogenous *Htr2c* was impeded by a transcriptional blocker cassette. Specific to this model, physiological levels of *Htr2c* can be restored selectively in distinct cell groups upon Cre recombinase activity. Consistent with previous reports (Nonogaki et al., 1998; Xu et al., 2008), chow-fed *Htr2c^{null}* mice were hyperphagic in a fasting-refeeding test but had body weight gains comparable with their wild-type littermates until 20 weeks of age because of a concomitant increase in energy expenditure (Figure S1A). However, hyperphagia was exacerbated when these mice were fed a high-fat diet (HFD; 42% kcal from fat, 0.2% cholesterol), tipping the scale of energy balance. As a result, despite the sustained higher energy expenditure, male *Htr2c^{null}* mice rapidly gained more weight and became significantly heavier than their littermate controls after an average of 8–10 weeks of HFD feeding (Figure 1A).

To examine whether selective restoration of *Htr2c* in *Sim1* neurons was sufficient to normalize the body weight deficits of *Htr2c^{null}* mice, we bred re-activatable *Htr2c^{nulll}* mice with *Sim1::Cre* mice (Balthasar et al., 2005) to generate *Htr2c^{null}, Sim1::Cre* mice in which endogenous levels of *Htr2c* were restored only in *Sim1* neurons (hereafter called *Htr2c^{Sim1RE}* mice). We found that

selective re-expression of *Htr2c* in *Sim1* neurons failed to normalize hyperphagia or higher energy expenditure in chow-fed mice (Figures S1B–S1D). In contrast, HFD-fed *Htr2c^{Sim1RE}* mice gained significantly more weight and became obese faster than their wild-type (*Sim1::Cre +/-*) and *Htr2c^{null}* littermates (Figure 1A). We then subjected another cohort of mice to a combined indirect calorimetry system (TSE metabolic chambers) where food intake, energy expenditure, and physical activity were monitored continuously. We found that, although the abnormal increase in energy expenditure persisted and remained comparable between HFD-fed *Htr2c^{null}* and *Htr2c^{Sim1RE}* mice (Figure 1B), hyperphagia was exaggerated in *Htr2c^{Sim1RE}* mice because they consumed significantly more calories than *Htr2c^{null}* mice during the dark phase, when mice are normally active (Figure 1C). The respiratory exchange ratio was not different among *Htr2c^{Sim1RE}*, *Htr2c^{null}*, and wild-type mice (Figure 1D).

Next we investigated whether *Htr2c* in *Sim1* neurons regulated the anorexigenic effects of serotonergic compounds such as dFen, a 5-HT releaser and uptake inhibitor, and meta-chlorophenylpiperazine (mCPP), a non-selective *Htr2c* agonist. Refeeding was measured in chow-fed mice after an overnight fast followed by an intraperitoneal (i.p.) dose of drug or saline. Despite the sustained effect on cumulative intake, the anorexigenic actions of dFen (6 mg/kg) and mCPP (5 mg/kg) were most prominent within the first 2 h following drug administration, whereas refeeding during subsequent hours was not statistically different between mice treated with drug or saline (Figures S1E–S1H). It has been reported previously reported that the anorexigenic effects of dFen and mCPP are blunted in conventional *Htr2c^{null}* mice (Tecott et al., 1995; Vickers et al., 1999). Similarly, we found that *Htr2c^{null}* mice showed attenuated anorectic responses to these agents (Xu et al., 2008). However, we unexpectedly found that such responses were blunted further in *Htr2c^{Sim1RE}* mice (Figures 1E and 1F). We then tested the response to lorcaserin, a selective agonist for *Htr2c* (Thomsen et al., 2008). As expected, lorcaserin (10 mg/kg) inhibited food intake in wild-type littermates but not in *Htr2c^{null}* mice (Figure 1G). Surprisingly, rather than suppressing food intake, lorcaserin appeared to increase food intake in *Htr2c^{Sim1RE}* mice (Figure 1G).

Selective ablation of *Htr2c* in *Sim1* neurons reduces food intake

Results from the re-expression studies raised the intriguing possibility that, despite its anorexigenic function in hypothalamic POMC neurons, *Htr2c* may act in *Sim1* neurons to promote food intake. To test this hypothesis, we selectively deleted *Htr2c* in *Sim1* neurons by breeding floxed *Htr2c* mice (Berglund et al., 2013) with *Sim1::Cre* mice to generate *Htr2c^{fl/Y}; Sim1::Cre* mice (hereafter called as *Htr2c^{Sim1KO}*). *Sim1::Cre* activity is enriched in neurons in the PVH and amygdala (Balthasar et al., 2005). *In situ* hybridization analyses demonstrated that *Htr2c* mRNAs were downregulated significantly in the PVH of *Htr2c^{Sim1KO}* mice, whereas levels within the amygdala were comparable between the two genotypes (Figures 2A–2D). Compared with their littermate controls (*Htr2c^{fl/Y}*), *Htr2c^{Sim1KO}* mice had normal body weight and body composition at 6 weeks of age (Figures 2E and 2F). Moreover, these mice demonstrated
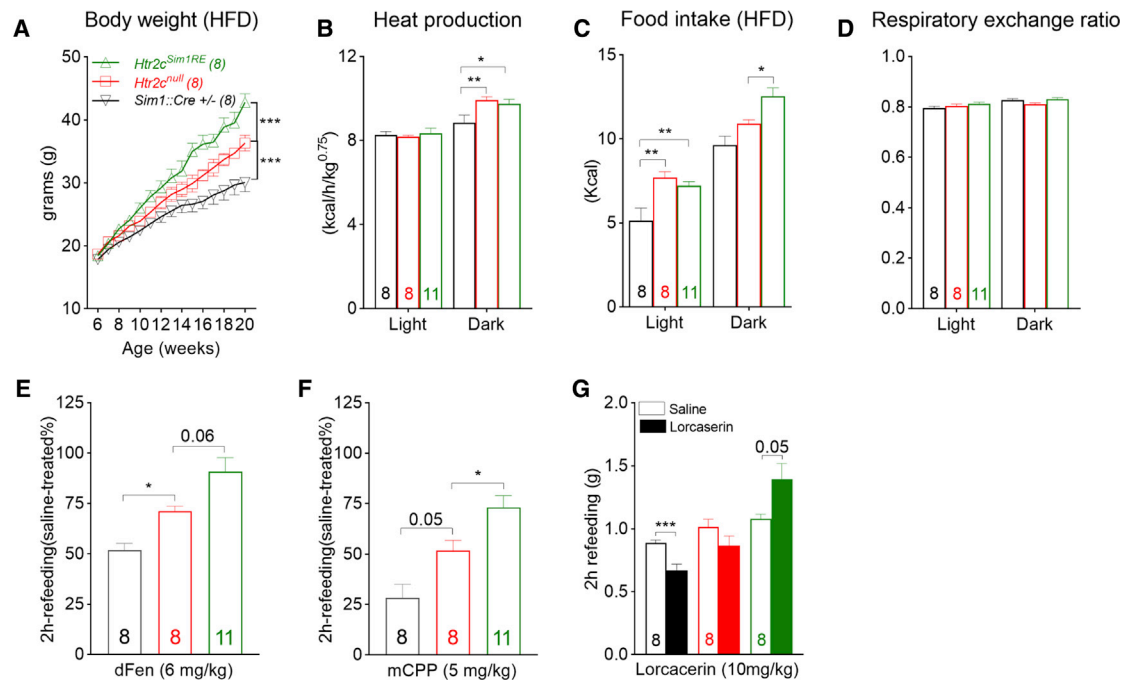
Figure 1. Restoration of *Htr2c* only in *Sim1* neurons increases food intake and body weight in male mice
(A) Body weight curves; $F_{(28, 294)} = 9.802$, $p < 0.001$.
(B) Heat production during light (06:00–18:00) and dark (18:00–06:00) phases of a day; $F_{(2, 24)} = 1.961$, $p = 0.16$.
(C and D) Food intake (C; $F_{(2, 24)} = 13$, $p < 0.001$) and (D) respiratory exchange ratio ($F_{(2, 24)} = 1.712$, $p = 0.2$) in HFD-fed male mice.
(E and F) Percentage of food intake (chow) after an i.p. dose of dFen (E, 6 mg/kg) or mCPP (F, 5 mg/kg), compared with vehicle-treated mice during the first 2 h of refeeding ($F_{(2, 24)} = 13.49$ and $F_{(2, 24)} = 14.5$ respectively; $p < 0.001$).
(G) Food intake (chow) after an i.p. dose of vehicle (saline) or lorcaserin during the first 2 h of refeeding; $p = 0.05$.
Values represent mean ± SEM; n = 8–11; two-way ANOVA with Tukey's post hoc tests in (A)–(D); one-way ANOVA with Tukey's post hoc tests in (E) and (F); paired t test in (G); *$p < 0.05$, **$p < 0.01$, ***$p < 0.001$.

normal glucoregulatory responses in glucose and insulin toler-ance tests (Figures S2A and S2B). However, *Htr2c^Sim1KO* mice gained less weight and became significantly leaner than their littermate controls when fed an HFD (Figure 2E). Nuclear mag-netic resonance analyses revealed that the decreased body weight in *Htr2c^Sim1KO* mice was due to a reduction in fat and lean mass (Figure 2F). Furthermore, metabolic chamber ana-lyses of a separate cohort of mice showed that food intake was reduced in HFD-fed *Htr2c^Sim1KO* mice (Figure 2G), whereas energy expenditure (Figure 2H) and physical activity (Figure 2I) remained comparable with their littermate controls. Interestingly, we found that chow-fed *Htr2c^Sim1KO* mice exhibited an anorectic response to a sub-anorectic dose of dFen (1 mg/kg) that otherwise did not suppress refeeding (during the first 2 h) in wild-type littermates (Figure 2J; Wurtman and Wurtman, 1977). Likewise, the anorectic response to mCPP (5 mg/kg) was also potentiated in these mice (Figure 2K). These findings suggest that *Htr2c* in *Sim1* neurons modulates the anorectic responses to 5-HT compounds.

PVH neurons are critical regulators of stress responses (Xu et al., 2019). Therefore, we investigated whether the observed decrease in food intake in *Htr2c^Sim1KO* mice was due to distress, such as increased anxiogenic and/or depressive behaviors. We tested two independent cohorts of control and *Htr2c^Sim1KO* mice that were fed chow (data not shown) or an HFD in a series of

behavioral paradigms including the elevated plus maze, dark-light exploration, open field tests for anxiety-related behaviors, as well as the forced swim test for depression-like behaviors (Figures S2C–S2F). However, we found no differences between the genotypes in any of these tests, indicating that the reduced food intake was unlikely to be the result of mood disturbances.

PVH *Htr2c* neurons bidirectionally regulate food intake

To investigate the neurochemical identity of PVH *Htr2c* neurons, we conducted Cre-mediated fate mapping using a *Htr2c::Cre* mouse we developed recently, in which expression of a Cre re-combinase is driven by the endogenous regulatory sequences of *Htr2c* (Park et al., 2020). We found that expression of a Cre-activated tdTomato reporter (Ai14) marked a subset of adult PVH neurons. None of these neurons expressed PVH neuronal markers such as oxytocin (OXY; Figure S3), arginine vasopressin (AVP), or tyrosine hydroxylase (TH). PVH neurons expressing *Mc4r* mediate the anorectic effect of serotonin downstream of *Htr2c*/POMC neurons (Xu et al., 2010). However, none of the to-mato-positive neurons in the PVH expressed *Mc4r*-GFP. Using double immunohistochemistry and *in situ* hybridization (Fig-ure S3), we found that the majority of PVH *Htr2c* neurons ex-pressed mRNAs for corticotropin-releasing hormone (*Crh*) or thyrotropin-releasing hormone (*Trh*). Furthermore, similar
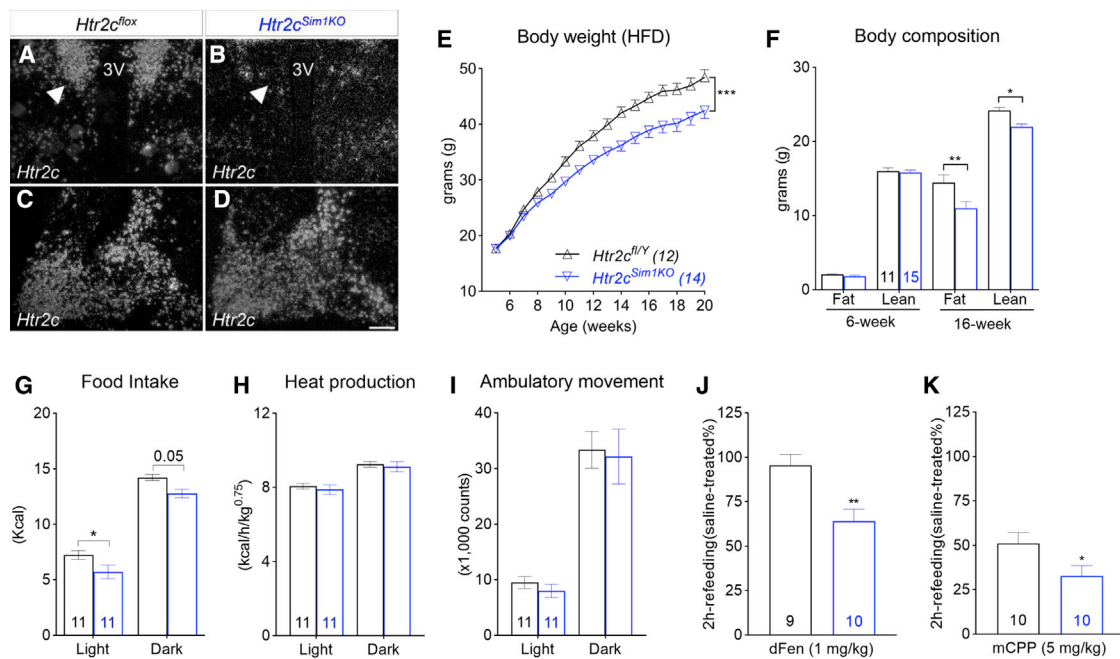
Figure 2. Selective deletion of *Htr2cs* in *Sim1* neurons reduces food intake and body weight in male mice

(A–D) *In situ* hybridization of *Htr2c* mRNA in the PVH (A and B) and amygdala (C and D) of *Htr2c*^{fl/Y} and *Htr2c*^{Sim1KO} mice.

(A–D) *In situ* hybridization of *Htr2c* mRNA in the PVH (A and B) and amygdala (C and D) of *Htr2c*^fl/Y^ and *Htr2c*^Sim1KO^ mice.

(E) Body weight curves; $F_{(15, 360)} = 4.78$, $p < 0.001$.

(F) Body composition; $F_{(3, 96)} = 3.91$, $p = 0.01$.

(G) Food intake during light and dark phases of a day; $F_{(1, 20)} = 13.44$, $p = 0.002$.

(H and I) Heat production (H; $F_{(1, 20)} = 0.33$, $p = 0.57$) and (I) physical activity ($F_{(1, 20)} = 0.16$, $p = 0.7$) in HFD-fed mice.

(J and K) Responses to dFen (J, 1 mg/kg) and mCPP (K, 5 mg/kg) in chow-fed *Htr2c*^fl/Y^ and *Htr2c*^Sim1KO^ mice.

Values represent mean ± SEM; n = 11–15, two-way ANOVA with Tukey's post hoc tests in (E)–(I); unpaired t tests in (J) and (K); *p < 0.05, **p < 0.01, ***p < 0.001.

---

analyses showed that these neurons did not express pituitary adenylate cyclase-activating polypeptide (*Pacap*) or galanin (*Gal*).

To test whether PVH *Htr2c* neurons directly regulate food intake *in vivo*, we stereotaxically delivered adeno-associated viruses (AAVs) expressing Cre-dependent Designer Receptors Exclusively Activated by Designer Drugs (DREADD) constructs (Krashes et al., 2011) into the PVH of *Htr2c::Cre* mice (Figures 3A and 3B). Following an i.p. dose of clozapine-N-oxide (CNO; 1 mg/kg), we found elevated levels of Fos protein, a marker for enhanced neuronal activity, on the ipsilateral side of the PVH that received the stimulatory DREADD (hM3Dq) (Figure 3C; 95.89 ± 6.18 positive cells/section compared with 14.56 ± 4.02 positive cells/section on the contralateral side). Fos expression was found in the majority (86.84% ± 4.25% of 469 cells from three mice) of *Htr2c* neurons that had been targeted by the GFP-labeled hM3Dq (Figure 3D). Consistent with this, electrophysiological recordings of GFP-labeled neurons showed that bath application of CNO (5 μM) elicited rapid depolarization of membrane potentials in PVH *Htr2c* neurons (Figures 3E and 3F). In *Htr2c::Cre* mice that received unilateral or bilateral hM3Dq injections in the PVH, a dose of CNO (i.p., 1 mg/kg) suppressed fasting-induced refeeding (Figure 3G). Importantly, CNO had no effect on food intake in mice in which the stereotaxic injections were placed outside of the PVH (misinjection; Fig-

ure 3G), nor did it alter feeding in *Htr2c::Cre* mice that received injections of a control virus (AAV-DIO-mCherry; Figure S4). Therefore, these findings demonstrate that chemogenetic activation of PVH *Htr2c* neurons inhibits feeding.

To evaluate the effect of silencing PVH *Htr2c* neurons on food intake, we conducted bilateral stereotaxic injections of AAVs that contained the inhibitory DREADD (hM4Di). Overnight-fasted mice were initially satiated for 1 h before receiving either CNO or saline. We found that individual mice consumed similar amounts of food during the satiation period (Figure 3H). However, compared with saline-treated mice, silencing PVH *Htr2c* neurons increased food intake after CNO treatment (Figure 3I). These findings demonstrated that PVH *Htr2c* neurons can bidirectionally regulate food intake *in vivo*. The effects of chemogenetic manipulations (stimulation or silencing) on food intake were transient because there were no differences in cumulative food intake between saline- and CNO-treated mice after 24 h (Figure S4).

Htr2c agonists hyperpolarize PVH neurons via postsynaptic K_{ATP} channels

Htr2c agonists hyperpolarize PVH neurons via postsynaptic K_{ATP} channels

Our chemogenetic experiments demonstrated that activation of PVH *Htr2c* neurons produced an anorectic effect. In contrast, our genetic studies appeared to suggest that *Htr2c* acts in PVH neurons to promote feeding. *Htr2c* has been reported to
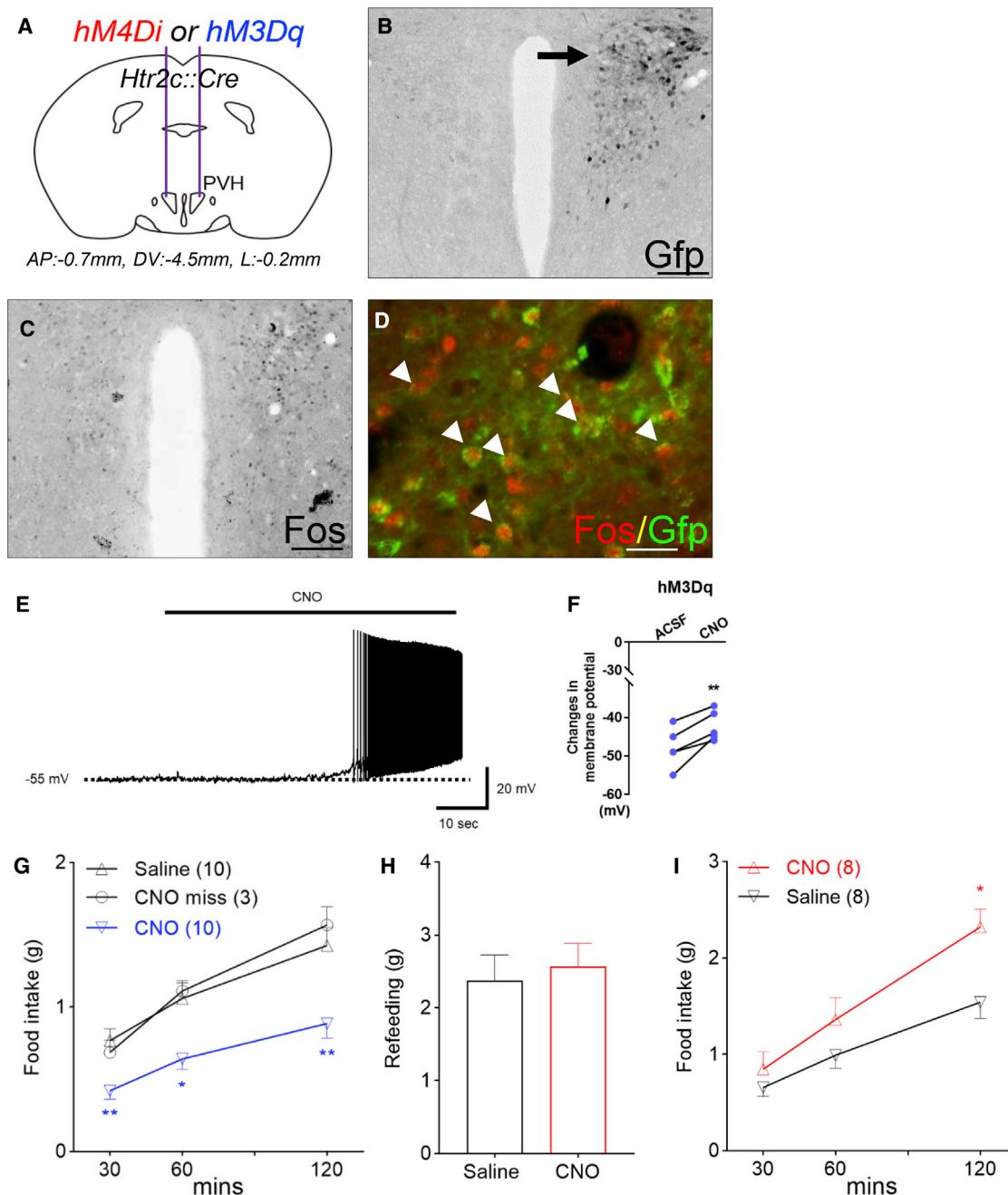
Figure 3. PVH *Htr2c* neurons directly regulate food intake in male mice
(A) Schematic for stereotaxic delivery of AAVs that contain stimulatory (hM3Dq) or inhibitory (hM4Di) DREADDs.
(B) Representative image showing unilateral targeting of GFP-labeled DREADD constructs in the PVH.
(C) Immunohistochemistry for Fos proteins.
(D) Double immunostaining for Fos and GFP. Arrowheads indicate double-labeled neurons.
(E) Bath application of CNO (5 μM) increased the firing rates of GFP-labeled PVH neurons.
(F) Change in membrane potentials.
(G) Stimulation of PVH *Htr2c* neurons suppressed fasting-induced refeeding; $F_{(2, 36)} = 3.511$, $p = 0.04$.
(H) Food intake during the 1-h satiation period after fasting.
(I) Silencing of PVH *Htr2c* neurons promoted feeding; $F_{(2, 28)} = 4.832$, $p = 0.002$.
Values represent mean ± SEM; *$p < 0.05$, **$p < 0.01$; two-way ANOVA with Sidak's post hoc tests in (F), (G), and (I). Scale bars, 200 μm (B and C) and 20 μm (D).

couple to the Gα_q/PLC pathway and, upon activation, to depolarize membrane potentials (Sohn et al., 2011). How could activation of *Htr2c* in anorexigenic PVH *Htr2c* neurons ultimately lead to an orexigenic effect? To investigate this apparent discrepancy, we studied the acute effects of *Htr2c* agonists on membrane potentials of genetically labeled *Htr2c* neurons in the arcuate nucleus of the hypothalamus (ARH) and the PVH.

We have demonstrated that activation of *Htr2c* depolarized a subset of ARH POMC neurons (Sohn et al., 2011). Consistent with this finding, mCPP (4 μM) depolarized a subpopulation of tomato-positive *Htr2c* neurons within the ARH (Figure S5). However, to our surprise, mCPP hyperpolarized the membrane potential of *Htr2c* neurons in the PVH by -9.9 ± 0.8 mV (28 of 76 cells, 36.8%; Figure 4A). The mCPP-induced hyperpolarization was not blunted by the presence of tetrodotoxin (TTX; 0.5 μM) and a cocktail of fast synaptic blockers (10 μM CNQX + 50 μM AP5 + 50 μM picrotoxin), supporting a postsynaptic event (-7.8 ± 0.9 mV, 6 of 11 cells, 54.5%; Figure 4B). We further tested the acute responses to the *Htr2c*-specific agonist lorcaserin and found that lorcaserin hyperpolarized PVH *Htr2c* neurons by -10.2 ± 2.2 mV (5 of 11 cells, 45.5%; Figure 4C). No depolarizing responses were recorded in the presence of mCPP (n = 76) or lorcaserin (n = 11). Moreover, lorcaserin-induced hyperpolarization of PVH *Htr2c* neurons was accompanied by an 18.6% ± 4.6% decrease in input resistance (from 1,074 ± 109 MΩ to 875 ± 103 MΩ, n = 5), which was comparable with that induced by mCPP treatment (decreased 20.5% ± 1.7% from 1,335 ± 53 MΩ to 1,056 ± 43 MΩ, n = 28). In both cases, the reversal potential (E_{rev}; -94.7 ± 7.1 mV for lorcaserin, -97.0 ± 2.4 mV for mCPP) was indicative of activated potassium conductance (Figure 4D). Consistent with these findings, we found that the mCPP-induced hyperpolarization in PVH *Htr2c* neurons was completely reversed by the ATP-sensitive K⁺ (K_{ATP}) channel inhibitors tolbutamide (200 μM; Figures 4A and 4E) and glibenclamide (100 μM; Figure 4F). Similarly, 5-HT (30 μM) hyperpolarized PVH *Htr2c* neurons (-9.2 ± 1.4 mV, 6 of 12 cells, 50.0%; Figures 4G and 4H), presumably by increasing potassium conductance (22.8% ± 1.4% decrease in input resistance from 1,571 ± 74 MΩ to 1,216 ± 71 MΩ, E_{rev} = -86.4 ± 4.5 mV, n = 6). Interestingly, we found that inhibition of Gα_q proteins/PLC signaling with anti-Gα_q antibodies or U73122 (a PLC inhibitor, 5 μM) failed to prevent mCPP-induced inhibition (Figures 4G and 4H, 11 of 26 cells [42.3%] pretreated with anti-Gα_q antibodies hyperpolarized by -7.7 ± 1.4 mV; 4 of 13 cells [30.8%] pretreated with U73122 hyperpolarized by -6.0 ± 1.1 mV, respectively). It has been reported that K_{ATP} channels can couple to the Gα_{i/o} pathway to hyperpolarize membrane potentials (Kurachi et al., 1992). In support of this, we found that application of pertussis toxin (PTX; 1 ng/μL), which inhibits Gα_{i/o} proteins, prevented mCPP-induced hyperpolarization of PVH *Htr2c* neurons (Figures 4G and 4H). These findings suggest that *Htr2c* couples to Gα_{i/o}-K_{ATP} pathway in PVH neurons to inhibit their activity and promote feeding.

DISCUSSION

Despite its pharmacological effect on appetite suppression, serotonergic regulation of feeding is far more complex at the physiological level. For example, dietary depletion of tryptophan,

a precursor of 5-HT biosynthesis, had little effect on food intake in healthy humans (Pagoto et al., 2009). Furthermore, mice completely lacking 5-HT in the brain or the whole body from early development are viable, fertile, and exhibit normal food intake and body weight (Mosienko et al., 2015). It has been shown that 5-HT can promote or inhibit food intake via different 5-HT receptors. For instance, its anorexigenic effect is largely attributed to activation of *Htr2c* and *Htr1b* (Lucas et al., 1998; Nonogaki et al., 1998). In contrast, treatment with 8-hydroxy-2-(di-n-propylamino) tetralin (8-OH-DPAT), an *Htr1a* agonist, increases feeding in C57BL/6 mice (Ebenezer and Surujbally, 2007).

Employing mouse genetic models in which endogenous *Htr2c* is selectively ablated or restored in *Sim1* neurons, our studies demonstrate that activation of *Htr2c* can produce orexigenic and anorexigenic effects. Similar to many other genes that are important for feeding regulation, *Htr2c* has broad distribution throughout the brain. Conventional wisdom has it that individual feeding regulators play coherent roles by promoting or inhibiting food intake at discrete central feeding nodes. Supporting this idea, the anorexigenic hormone leptin suppresses food intake by activating anorexigenic POMC neurons and inhibiting orexigenic AgRP neurons (Baver et al., 2014; Cowley et al., 2001; Hill et al., 2008). However, our study reveals that activation of *Htr2c* at different brain sites can have opposing effects on food intake. Contrary to its anorexigenic role in POMC neurons, *Htr2c* acts in *Sim1* neurons to promote food intake. This is further supported by our findings that restoration of *Htr2c* only in *Sim1* neurons exacerbates hyperphagia in *Htr2c*^{null} mice, whereas its selective deletion in the same neurons reduces food intake. Along this line, we show that the pharmacological effects of 5-HT agents can be differentially modulated by *Htr2c* in different brain locations. Opposite to its effect in POMC neurons, we find that *Htr2c* acts in *Sim1* neurons to dampen anorectic responses. This is corroborated by the observation that lorcaserin, an *Htr2c*-specific agonist, suppressed feeding in wild-type animals but appeared to increase food intake in mice in which *Htr2c* was expressed exclusively in *Sim1* neurons. We hypothesize that *Htr2c* in *Sim1* neurons may provide important regulatory feedback that restricts the effectiveness and safety of serotonergic appetite suppressants. Moreover, these data may be a cellular correlate to the rather modest anti-obesity effects of lorcaserin that have been observed in humans (Tchang et al., 2020).

Sim1::Cre activity has been reported only in a handful of brain structures, including most prominently the PVH and medial amygdala (Balthasar et al., 2005). Our observation that *Htr2c* expression was largely preserved in the amygdala of *Htr2c*^{Sim1KO} mice suggests minimal overlap between *Sim1::Cre* and *Htr2c* expression in the amygdala and that the reduced food intake in these mice was not likely to be due to loss of amygdala *Htr2c*. These findings implicate the PVH as another critical brain site where *Htr2c* regulates food intake. Importantly, reactivation or deletion of *Htr2c* in *Sim1* neurons had no effect on other physiological processes, such as energy expenditure, physical activity, or glucose homeostasis. Furthermore, mice lacking *Htr2c* in *Sim1* neurons had normal responses in a battery of anxiety- and depression-related behavioral tests. Our findings suggest a dedicated role of *Htr2c* in *Sim1* neurons for feeding regulation.
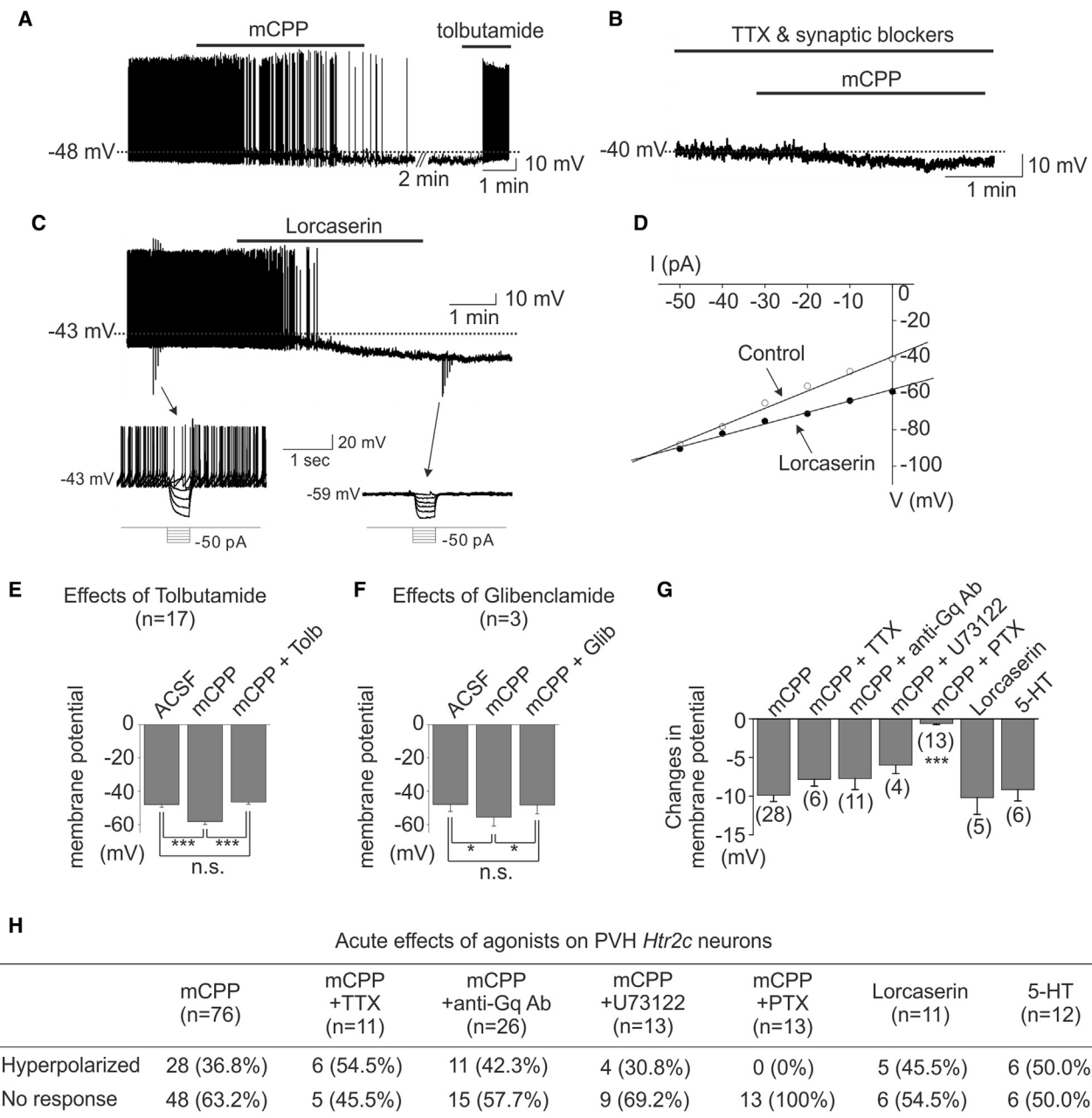
Figure 4. Activation of *Ht2c* hyperpolarizes PVH *Htr2c* neurons

(A) Bath applications of mCPP caused prompt hyperpolarization of membrane potential, which was completely reversed by subsequent applications of tolbutamide.

(B) mCPP-induced hyperpolarization was not affected by addition of TTX and fast synaptic blockers in the bath solutions.

(C) Bath applications of lorcaserin, an *Htr2c*-specific agonist, caused prompt hyperpolarization of membrane potential. Downward deflections shown in the trace represent voltage responses to current steps, which are shown as insets below.

(D) Current-voltage (IV) relationship before (control) and after drug (lorcaserin) application. The E_{rev} is close to the equilibrium potential for K^+ (E_K).

(E) Bar graphs summarizing the effects of tolbutamide on mCPP-induced hyperpolarization.

(F) Bar graphs summarizing the effects of glibenclamide.

(G) Bar graphs showing the average amplitude of mCPP-, lorcaserin-, or 5-HT-induced hyperpolarization.

(H) Table summarizing the numbers and percentages of the responses to mCPP treatment in recorded *Htr2c* neurons within the PVH.

Values represent mean ± SEM; *p < 0.05, ***p < 0.001; repeated-measures two-way ANOVA with Tukey's or Bonferroni's post hoc test in (E)–(G).

Delineation of PVH feeding circuits is a challenge because the PVH consists of several functionally heterogeneous neuronal populations that differ in morphology, connectivity, and peptidergic identity (Biag et al., 2012; Swanson and Sawchenko, 1983). Our immunohistochemical analyses demonstrated that *Htr2c* marks a distinct population of PVH neurons that largely consist of subsets of parvocellular CRH and TRH neurons. These findings are in agreement with earlier histological data showing that 5-HT terminals in the PVH are enriched in the parvocellular division of the nucleus (Sawchenko et al., 1983). Likewise, numerous studies have established an inhibitory role of PVH neurons in food intake. With few exceptions (Krashes et al., 2014), activation of PVH neurons typically leads to suppression of food intake, whereas silencing or genetic ablation of these neurons causes hyperphagia (An et al., 2020; Atasoy et al., 2012; Li et al., 2019; Liu et al., 2017; Pei et al., 2014; Xi et al., 2013). Consistent with the anorexigenic effect of CRH and TRH (Krahn et al., 1988; Vijayan and McCann, 1977), we found that adult chemogenetic stimulation of PVH *Htr2c* neurons suppressed hunger-induced refeeding, whereas silencing of these neurons boosted consumption in satiated mice. These findings establish that PVH *Htr2c* neurons can bidirectionally regulate food intake *in vivo*. However, future studies are warranted to map the serotonergic inputs and downstream targets of these neurons. We have shown previously that PVH MC4Rs act downstream of the ARH *Htr2c*/POMC neurons to mediate the anorectic effect of 5-HT agents (Xu et al., 2010). Interestingly, PVH *Htr2c* neurons do not express MC4R-GFP. Furthermore, it has been shown that different hypothalamic nuclei are innervated by discrete serotonergic cell groups in the midbrain (Sawchenko et al., 1983). Therefore, we predict that *Htr2c* neurons in the ARH and PVH may receive inputs from discrete 5-HT neurons and activate under different physiological conditions.

Htr2c regulates food intake through homeostatic and non-homeostatic mechanisms. For example, dopamine (DA) neurons in the ventral tegmental area (VTA) express *Htr2c* and are activated by its specific agonist, lorcaserin (Xu et al., 2017). Given the importance of DA neurons in reward processing, *Htr2c* may regulate hedonic feeding in part through VTA DA neurons. In support of this notion, loss of *Htr2c* in these neurons attenuates lorcaserin's inhibitory effect on binge-like eating but does not alter its anorectic effect on hunger-driven feeding (Xu et al., 2017). In the current study, we found that chow-fed *Htr2c*^nulll and *Htr2c*^Sim1RE mice were hyperphagic but had comparable food intake in a fasting-refeeding paradigm. In contrast, *Htr2c*^Sim1RE mice consumed more food than *Htr2c*^nulll mice when both were fed an HFD. Consistent with this finding, HFD-fed *Htr2c*^Sim1KO mice ate less than controls and were protected from HFD-induced weight gain. These findings support a role of *Htr2c* in *Sim1* neurons in HFD-induced feeding adaptations. Many PVH *Htr2c* neurons express CRH, and a recent study has reported that reward consumption of sucrose solution inhibits PVH CRH neurons in freely behaving mice (Yuan et al., 2019). Although we showed that chemogenetic inhibition of PVH *Htr2c* neurons was sufficient to increase food intake in mice, future studies are warranted to determine whether HFD consumption has a similar inhibitory effect on PVH CRH neurons and whether it induces hyperphagia by inhibiting PVH CRH/*Htr2c* neurons.

Htr2c has been known to couple to the Gαq pathway and, upon activation, is expected to increase neuronal activity. In support of this, we demonstrated previously that *Htr2c* agonists depolarized ARH POMC neurons in a Gαq/PLC-dependent manner (Sohn et al., 2011). In the current study, we verified this finding and found that mCPP depolarized genetically labeled *Htr2c*/POMC neurons in the ARH of triple-transgenic *Htr2c::Cre, R26R::tdTomato, Pomc::GFP* mice. However, recordings in the same mice revealed that none of the PVH *Htr2c* neurons showed a depolarizing response to *Htr2c* agonist treatment. In contrast, half of them were hyperpolarized by mCPP or lorcaserin. These findings, along with the observation that adult inhibition of PVH *Htr2c* neurons increased food intake, corroborated the reactivation/deletion experiments and demonstrated that activation of PVH *Htr2c* promotes feeding. We further demonstrated that hyperpolarization of PVH neurons involved opening of postsynaptic K_ATP conductance. Most surprisingly, however, neither pretreatment with anti-Gα_q antibodies nor a PLC inhibitor prevented *Htr2c*-mediated inhibition. Instead, it was blocked by the Gα_i/o-sensitive PTX. Although functional coupling between *Htr2c* and Gα_i/o has been described previously in *Xenopus* oocytes (Chen et al., 1994; Lucaites et al., 1996), we present evidence that this mechanism is important in the mammalian nervous system. These findings suggest that *Htr2c* can differentially regulate neuronal excitability and food intake in different neurons by coupling with distinct intracellular signaling events.

Limitations of the study

Our study utilizes sophisticated mouse genetic models in which *Htr2c* is selectively deleted or restored in *Sim1::Cre* neurons during early life. However, whether developmental manipulations of gene expression could have contributed to the observed phenotypes in adult mice remains unknown. We also cannot rule out the possibility that alterations in *Htr2c* expression in *Sim1::Cre* neurons may cause changes in gene transcription in these neurons or in other brain regions. Additionally, we use a *Htr2c::Cre* activated tdTomato reporter to mark *Htr2c*-expressing neurons in the PVH. Although we have validated this genetic tool in a previous study (Park et al., 2020), it may not capture the entire *Htr2c* neuron population. Finally, we use a chemogenetic approach to demonstrate that PVH *Htr2c* neurons are sufficient to drive feeding behaviors *in vivo*. Although this type of approach has been used in many studies, these manipulations may not recapitulate the normal physiological changes in the activity of PVH *Htr2c* neurons.

STAR★METHODS

Detailed methods are provided in the online version of this paper and include the following:

- KEY RESOURCES TABLE
- RESOURCE AVAILABILITY
    - Lead contact
    - Materials availability
    - Data and code availability
- EXPERIMENTAL MODEL AND SUBJECT DETAILS

- ○ Mice
- ● METHOD DETAILS
  - ○ Body weight and composition
  - ○ Metabolic cage studies
  - ○ Behavioral analyses
  - ○ Response to d-Fen, mCPP, and lorcaserin
  - ○ Blood glucose, glucose, and insulin tolerance tests
  - ○ Histology
  - ○ Electrophysiology
  - ○ Stereotaxic injections
- ● QUANTIFICATION AND STATISTICAL ANALYSIS

REFERENCES

An, J.J., Kinney, C.E., Tan, J.W., Liao, G.Y., Kremer, E.J., and Xu, B. (2020). TrkB-expressing paraventricular hypothalamic neurons suppress appetite through multiple neurocircuits. Nat. Commun. 11, 1729.

Atasoy, D., Betley, J.N., Su, H.H., and Sternson, S.M. (2012). Deconstruction of a neural circuit for hunger. Nature 488, 172–177.

Balthasar, N., Dalgaard, L.T., Lee, C.E., Yu, J., Funahashi, H., Williams, T., Ferreira, M., Tang, V., McGovern, R.A., Kenny, C.D., et al. (2005). Divergence of melanocortin pathways in the control of food intake and energy expenditure. Cell 123, 493–505.

Baver, S.B., Hope, K., Guyot, S., Bjørbaek, C., Kaczorowski, C., and O'Connell, K.M. (2014). Leptin modulates the intrinsic excitability of AgRP/NPY neurons in the arcuate nucleus of the hypothalamus. J. Neurosci. 34, 5486–5496.

Berglund, E.D., Liu, C., Sohn, J.W., Liu, T., Kim, M.H., Lee, C.E., Vianna, C.R., Williams, K.W., Xu, Y., and Elmquist, J.K. (2013). Serotonin 2C receptors in pro-opiomelanocortin neurons regulate energy and glucose homeostasis. J. Clin. Invest. 123, 5061–5070.

Betley, J.N., Cao, Z.F., Ritola, K.D., and Sternson, S.M. (2013). Parallel, redundant circuit organization for homeostatic control of feeding behavior. Cell 155, 1337–1350.

Biag, J., Huang, Y., Gou, L., Hintiryan, H., Askarinam, A., Hahn, J.D., Toga, A.W., and Dong, H.W. (2012). Cyto- and chemoarchitecture of the hypothalamic paraventricular nucleus in the C57BL/6J male mouse: a study of immunostaining and multiple fluorescent tract tracing. J. Comp. Neurol. 520, 6–33.

Cai, H., Haubensak, W., Anthony, T.E., and Anderson, D.J. (2014). Central amygdala PKC-δ(+) neurons mediate the influence of multiple anorexigenic signals. Nat. Neurosci. 17, 1240–1248.

Cetin, A., Komai, S., Eliava, M., Seeburg, P.H., and Osten, P. (2006). Stereotaxic gene delivery in the rodent brain. Nat. Protoc. 1, 3166–3173.

Chen, Y., Baez, M., and Yu, L. (1994). Functional coupling of the 5-HT2C serotonin receptor to G proteins in Xenopus oocytes. Neurosci. Lett. 179, 100–102.

Colman, E., Golden, J., Roberts, M., Egan, A., Weaver, J., and Rosebraugh, C. (2012). The FDA's assessment of two drugs for chronic weight management. N. Engl. J. Med. 367, 1577–1579.

Cowley, M.A., Smart, J.L., Rubinstein, M., Cerdán, M.G., Diano, S., Horvath, T.L., Cone, R.D., and Low, M.J. (2001). Leptin activates anorexigenic POMC neurons through a neural network in the arcuate nucleus. Nature 411, 480–484.

D'Agostino, G., Lyons, D., Cristiano, C., Lettieri, M., Olarte-Sanchez, C., Burke, L.K., Greenwald-Yarnell, M., Cansell, C., Doslikova, B., Georgescu, T., et al. (2018). Nucleus of the Solitary Tract Serotonin 5-HT$_{2C}$ Receptors Modulate Food Intake. Cell Metab. 28, 619–630.e5.

Ebenezer, I.S., and Surujbally, A. (2007). The effects of 8-hydroxy-2-(di-n-propylamino)-tetralin (8-OH-DPAT) on food intake in non-deprived C57BL6 mice. Eur. J. Pharmacol. 559, 184–188.

Fyffe, S.L., Neul, J.L., Samaco, R.C., Chao, H.T., Ben-Shachar, S., Moretti, P., McGill, B.E., Goulding, E.H., Sullivan, E., Tecott, L.H., and Zoghbi, H.Y. (2008). Deletion of Mecp2 in Sim1-expressing neurons reveals a critical role for MeCP2 in feeding behavior, aggression, and the response to stress. Neuron 59, 947–958.

Heisler, L.K., Pronchuk, N., Nonogaki, K., Zhou, L., Raber, J., Tung, L., Yeo, G.S., O'Rahilly, S., Colmers, W.F., Elmquist, J.K., and Tecott, L.H. (2007). Serotonin activates the hypothalamic-pituitary-adrenal axis via serotonin 2C receptor stimulation. J. Neurosci. 27, 6956–6964.

Hill, J.W., Williams, K.W., Ye, C., Luo, J., Balthasar, N., Coppari, R., Cowley, M.A., Cantley, L.C., Lowell, B.B., and Elmquist, J.K. (2008). Acute effects of leptin require PI3K signaling in hypothalamic proopiomelanocortin neurons in mice. J. Clin. Invest. 118, 1796–1805.

Hoffman, B.J., and Mezey, E. (1989). Distribution of serotonin 5-HT1C receptor mRNA in adult rat brain. FEBS Lett. 247, 453–462.

Holder, J.L., Jr., Zhang, L., Kublaoui, B.M., DiLeone, R.J., Oz, O.K., Bair, C.H., Lee, Y.H., and Zinn, A.R. (2004). Sim1 gene dosage modulates the homeostatic feeding response to increased dietary fat in mice. Am. J. Physiol. Endocrinol. Metab. 287, E105–E113.

Kenny, P.J. (2011). Reward mechanisms in obesity: new insights and future directions. Neuron 69, 664–679.

Krahn, D.D., Gosnell, B.A., Levine, A.S., and Morley, J.E. (1988). Behavioral effects of corticotropin-releasing factor: localization and characterization of central effects. Brain Res. 443, 63–69.

Krashes, M.J., Koda, S., Ye, C., Rogan, S.C., Adams, A.C., Cusher, D.S., Maratos-Flier, E., Roth, B.L., and Lowell, B.B. (2011). Rapid, reversible activation of AgRP neurons drives feeding behavior in mice. J. Clin. Invest. 121, 1424–1428.

Krashes, M.J., Shah, B.P., Madara, J.C., Olson, D.P., Strochlic, D.E., Garfield, A.S., Vong, L., Pei, H., Watabe-Uchida, M., Uchida, N., et al. (2014). An excitatory paraventricular nucleus to AgRP neuron circuit that drives hunger. Nature 507, 238–242.

Kurachi, Y., Tung, R.T., Ito, H., and Nakajima, T. (1992). G protein activation of cardiac muscarinic K+ channels. Prog. Neurobiol. 39, 229–246.

Li, M.M., Madara, J.C., Steger, J.S., Krashes, M.J., Balthasar, N., Campbell, J.N., Resch, J.M., Conley, N.J., Garfield, A.S., and Lowell, B.B. (2019). The

Paraventricular Hypothalamus Regulates Satiety and Prevents Obesity via Two Genetically Distinct Circuits. Neuron *102*, 653–667.e6.

Li, L., Yoo, E.S., Li, X., Wyler, S.C., Chen, X., Wan, R., Arnold, A.G., Birnbaum, S.G., Jia, L., Sohn, J.W., and Liu, C. (2021). The atypical antipsychotic risperidone targets hypothalamic melanocortin 4 receptors to cause weight gain. J. Exp. Med. *218*, e20202484.

Liu, C., Maejima, T., Wyler, S.C., Casadesus, G., Herlitze, S., and Deneris, E.S. (2010). Pet-1 is required across different stages of life to regulate serotonergic function. Nat. Neurosci. *13*, 1190–1198.

Liu, J., Conde, K., Zhang, P., Lilascharoen, V., Xu, Z., Lim, B.K., Seeley, R.J., Zhu, J.J., Scott, M.M., and Pang, Z.P. (2017). Enhanced AMPA Receptor Trafficking Mediates the Anorexigenic Effect of Endogenous Glucagon-like Peptide-1 in the Paraventricular Hypothalamus. Neuron *96*, 897–909.e5.

Lucaites, V.L., Nelson, D.L., Wainscott, D.B., and Baez, M. (1996). Receptor subtype and density determine the coupling repertoire of the 5-HT2 receptor subfamily. Life Sci. *59*, 1081–1095.

Lucas, J.J., Yamamoto, A., Scearce-Levie, K., Saudou, F., and Hen, R. (1998). Absence of fenfluramine-induced anorexia and reduced c-Fos induction in the hypothalamus and central amygdaloid complex of serotonin 1B receptor knock-out mice. J. Neurosci. *18*, 5537–5544.

Michaud, J.L., Boucher, F., Melnyk, A., Gauthier, F., Goshu, E., Lévy, E., Mitchell, G.A., Himms-Hagen, J., and Fan, C.M. (2001). Sim1 haploinsufficiency causes hyperphagia, obesity and reduction of the paraventricular nucleus of the hypothalamus. Hum. Mol. Genet. *10*, 1465–1473.

Mosienko, V., Beis, D., Pasqualetti, M., Waider, J., Matthes, S., Qadri, F., Bader, M., and Alenina, N. (2015). Life without brain serotonin: reevaluation of serotonin function with mice deficient in brain serotonin synthesis. Behav. Brain Res. *277*, 78–88.

Nonogaki, K., Strack, A.M., Dallman, M.F., and Tecott, L.H. (1998). Leptin-independent hyperphagia and type 2 diabetes in mice with a mutated serotonin 5-HT2C receptor gene. Nat. Med. *4*, 1152–1156.

Pagoto, S.L., Spring, B., McChargue, D., Hitsman, B., Smith, M., Appelhans, B., and Hedeker, D. (2009). Acute tryptophan depletion and sweet food consumption by overweight adults. Eat. Behav. *10*, 36–41.

Park, S., Williams, K.W., Liu, C., and Sohn, J.W. (2020). A neural basis for tonic suppression of sodium appetite. Nat. Neurosci. *23*, 423–432.

Pei, H., Sutton, A.K., Burnett, K.H., Fuller, P.M., and Olson, D.P. (2014). AVP neurons in the paraventricular nucleus of the hypothalamus regulate feeding. Mol. Metab. *3*, 209–215.

Sawchenko, P.E., Swanson, L.W., Steinbusch, H.W., and Verhofstad, A.A. (1983). The distribution and cells of origin of serotonergic inputs to the paraventricular and supraoptic nuclei of the rat. Brain Res. *277*, 355–360.

Schwartz, G.J., and Zeltser, L.M. (2013). Functional organization of neuronal and humoral signals regulating feeding behavior. Annu. Rev. Nutr. *33*, 1–21.

Sohn, J.W., Xu, Y., Jones, J.E., Wickman, K., Williams, K.W., and Elmquist, J.K. (2011). Serotonin 2C receptor activates a distinct population of arcuate pro-opiomelanocortin neurons via TRPC channels. Neuron *71*, 488–497.

Swanson, L.W., and Sawchenko, P.E. (1983). Hypothalamic integration: organization of the paraventricular and supraoptic nuclei. Annu. Rev. Neurosci. *6*, 269–324.

Tchang, B.G., Abel, B., Zecca, C., Saunders, K.H., and Shukla, A.P. (2020). An up-to-date evaluation of lorcaserin hydrochloride for the treatment of obesity. Expert Opin. Pharmacother. *21*, 21–28.

Tecott, L.H., Sun, L.M., Akana, S.F., Strack, A.M., Lowenstein, D.H., Dallman, M.F., and Julius, D. (1995). Eating disorder and epilepsy in mice lacking 5-HT2c serotonin receptors. Nature *374*, 542–546.

Thomsen, W.J., Grottick, A.J., Menzaghi, F., Reyes-Saldana, H., Espitia, S., Yuskin, D., Whelan, K., Martin, M., Morgan, M., Chen, W., et al. (2008). Lorcaserin, a novel selective human 5-hydroxytryptamine2C agonist: in vitro and in vivo pharmacological characterization. J. Pharmacol. Exp. Ther. *325*, 577–587.

Vianna, C.R., Donato, J., Jr., Rossi, J., Scott, M., Economides, K., Gautron, L., Pierpont, S., Elias, C.F., and Elmquist, J.K. (2012). Cannabinoid receptor 1 in the vagus nerve is dispensable for body weight homeostasis but required for normal gastrointestinal motility. J. Neurosci. *32*, 10331–10337.

Vickers, S.P., Clifton, P.G., Dourish, C.T., and Tecott, L.H. (1999). Reduced satiating effect of d-fenfluramine in serotonin 5-HT(2C) receptor mutant mice. Psychopharmacology (Berl.) *143*, 309–314.

Vijayan, E., and McCann, S.M. (1977). Suppression of feeding and drinking activity in rats following intraventricular injection of thyrotropin releasing hormone (TRH). Endocrinology *100*, 1727–1730.

Wurtman, J.J., and Wurtman, R.J. (1977). Fenfluramine and fluoxetine spare protein consumption while suppressing caloric intake by rats. Science *198*, 1178–1180.

Wyler, S.C., Lord, C.C., Lee, S., Elmquist, J.K., and Liu, C. (2017). Serotonergic Control of Metabolic Homeostasis. Front. Cell. Neurosci. *11*, 277.

Xi, D., Roizen, J., Lai, M., Gandhi, N., and Kublaoui, B. (2013). Paraventricular nucleus Sim1 neuron ablation mediated obesity is resistant to high fat diet. PLoS ONE *8*, e81087.

Xu, Y., Jones, J.E., Kohno, D., Williams, K.W., Lee, C.E., Choi, M.J., Anderson, J.G., Heisler, L.K., Zigman, J.M., Lowell, B.B., and Elmquist, J.K. (2008). 5-HT2CRs expressed by pro-opiomelanocortin neurons regulate energy homeostasis. Neuron *60*, 582–589.

Xu, Y., Jones, J.E., Lauzon, D.A., Anderson, J.G., Balthasar, N., Heisler, L.K., Zinn, A.R., Lowell, B.B., and Elmquist, J.K. (2010). A serotonin and melanocortin circuit mediates D-fenfluramine anorexia. J. Neurosci. *30*, 14630–14634.

Xu, P., He, Y., Cao, X., Valencia-Torres, L., Yan, X., Saito, K., Wang, C., Yang, Y., Hinton, A., Jr., Zhu, L., et al. (2017). Activation of Serotonin 2C Receptors in Dopamine Neurons Inhibits Binge-like Eating in Mice. Biol. Psychiatry *81*, 737–747.

Xu, Y., Lu, Y., Cassidy, R.M., Mangieri, L.R., Zhu, C., Huang, X., Jiang, Z., Justice, N.J., Xu, Y., Arenkiel, B.R., and Tong, Q. (2019). Identification of a neurocircuit underlying regulation of feeding by stress-related emotional responses. Nat. Commun. *10*, 3446.

Yuan, Y., Wu, W., Chen, M., Cai, F., Fan, C., Shen, W., Sun, W., and Hu, J. (2019). Reward Inhibits Paraventricular CRH Neurons to Relieve Stress. Curr. Biol. *29*, 1243–1251.e4.

Cell Reports
Report

STAR★METHODS

KEY RESOURCES TABLE

REAGENT	SOURCE	IDENTIFIER
Antibodies		
Anti- oxytocin	Abcam	RRID: AB_302818, Cat# ab2078
Anti- arginine vasopressin	Thermo Scientific	RRID: AB_11003086, Cat# PA5-19819
Anti- tyrosine hydroxylase	Abcam	RRID: AB_297840, Cat# ab112
Anti-c-Fos	Santa Cruz	RRID: AB_2629503, Cat# sc-52-G
Anti- GFP	Life Technologies	RRID: AB_221570, Cat# A6455
Anti-Gq/11α	Merck Millipore	RRID: AB_310221, Cat# 06-709
Bacterial and virus strains		
hSyn-DIO-mCherry	Addgene plasmid	RRID:Addgene_50459, Cat# 50459
hSyn-DIO-hM3D(Gq)-mCherry	Addgene plasmid	RRID:Addgene_44361, Cat# 44361
hSyn-DIO-hM4D(Gi)-mCherry	Addgene plasmid	RRID:Addgene_44362, Cat# 44362
Chemicals, peptides, and recombinant proteins		
Insulin (Humulin)	Lilly	Cat# HI-210
Dextrose 50% Solution	Hospira	Cat# 00409-6648-02
D-Fen	Sigma	Cat #F112
mCPP	Sigma	Cat #C-089
Lorcaserin	A gift from Dr. Kathryn A. Cunningham	N/A
Chloral hydrate	Sigma	Cat #C8383
Sucrose	Sigma	Cat #S0389
CNO	Sigma	Cat #SML2304
CNQX disodium salt	Tocris	Cat #1045
DL-AP5	Tocris	Cat #0105
Picrotoxin	Tocris	Cat #1128
TTX citrate	Tocris	Cat #1069
U73122	Tocris	Cat #1268
Pertussis toxin	Tocris	Cat #3097
5-HT	Tocris	Cat #3547
Tolbutamide	Sigma	Cat #T0891
Glibenclamide	Sigma	Cat #G0639
Rodent Diet With 42 kcal% Fat	Harlan Teklad	Cat# 88137
Standard chow	Harlan Teklad	Cat# 2916
Experimental models: Organisms/strains		
Mouse: C57BL/6J	The Jackson Laboratory	RRID: JAX:000664
Mouse: Sim1::Cre	Bradford B Lowell	RRID: MGI:3692526
Mouse: Htr2c::Cre	Chen Liu	Park et al., 2020
Mouse: Htr2c^{null}	Joel K Elmquist	RRID: MGI:3841486
Mouse: Htr2c^{flox}	Joel K Elmquist	RRID: MGI:5569357
Mouse: Gt(ROSA)26Sor$^{(RCL-tdT)-D}$ (Ai14)	The Jackson Laboratory	RRID: JAX: 007914
Oligonucleotides		
See Table S1 for oligo nucleotide information		N/A
Other		
Indirect calorimetry system – TSE PhenoMaster	TSE Systems Germany	N/A
EchoMRI	EchoMRI Corporation	N/A

(Continued on next page)

Continued		
REAGENT	SOURCE	IDENTIFIER
Vibratome	Leica	N/A
Glucometer	AlphaTrak	N/A
GraphPad version 9	GraphPad Software Inc	https://www.graphpad.com

RESOURCE AVAILABILITY

Lead contact
Further information and requests for resources and reagents should be directed to the lead contact, Chen Liu (chen.liu@utsouthwestern.edu).

Materials availability
No new unique reagents were generated in this study. Reagents will be made available upon completion of a Material Transfer Agreement.

Data and code availability

- All data reported in this paper will be shared by the lead contact upon request.
- This paper does not report original code.
- Any additional information required to reanalyze the data reported in this paper is available from the lead contact upon request.

EXPERIMENTAL MODEL AND SUBJECT DETAILS

All experimental procedures were approved by the Institutional Animal Care and Use Committee (IACUC) at the University of Texas Southwestern Medical Center and Korea Advanced Institute of Science and Technology.

Mice
All mice were housed in a temperature-controlled room with a twelve-hour-light/dark cycle (lights on at 06:00 a.m., lights off at 6:00 p.m.) in the animal facility of the University of Texas Southwestern Medical Center at Dallas. Food and water were supplied *ad libitum*. Mice were fed with either regular chow (#2916, Harlan-Teklad, Madison, WI; 4.25% kcal from fat) or a high-fat diet (HFD, #88137, Harlan Teklad, 42% kcal from fat). $Htr2c^{RN/Y}$; Sim1::Cre ± , $Htr2c^{RN/Y}$, and $Htr2c^{+/Y}$; Sim1::Cre ± mice were maintained on a C57BL/6 background, whereas $Htr2c^{fl/Y}$; Sim1::Cre and $Htr2c^{fl/Y}$ mice were on a mixed C57BL/6 × 129 background. Htr2c::Cre mice were generated by conventional gene targeting in mouse embryonic stem cells.

METHOD DETAILS

Body weight and composition
Body weight was monitored weekly from weaning (four-week-old) to twenty-five weeks of age. In the HFD studies, mice were maintained on regular chow until six weeks old before being fed HFD. Body composition was assessed using the Bruker Minispec mq10 NMR analyzer at six and sixteen weeks of age.

Metabolic cage studies
Data for food intake, meal patterns, energy expenditure, and physical activities were collected using a combined indirect calorimetry system (TSE Systems GmbH, Bad Homburg, Germany). Experimental animals were individually acclimated in the metabolic chambers for five days before data collection. During data collection, mice were initially fed the chow diet in the first two days of data collection and switched to the HFD diet for the next three days in the metabolic cages.

Behavioral analyses
All tests were carried out in the UTSW Rodent Behavior Core. Elevated plus maze, dark light exploration, open field, and forced swim tests were conducted as previously described (Liu et al., 2010). At least two independent cohorts of mice were tested in all of the behavioral paradigms. All tests were conducted during the light cycle of the day between 10:30 am and 6:00 pm. All equipment was cleaned thoroughly with 70% ethanol between individual tests to remove odor cues. Individual behavioral experiments were performed at least forty-eight hours apart from one another. The tester/scorer was blind to genotype identification.

Response to d-Fen, mCPP, and lorcaserin

We measured food intake in overnight-fasted mice hourly (up to six hours) after an intraperitoneal dose of D-Fen (6 mg/kg; Sigma-Aldrich), mCPP (3 mg/kg; Sigma-Aldrich), lorcaserin (10 mg/kg, a gift from Dr. Kathryn A. Cunningham) or sterile saline. Drugs and saline were administered in a counterbalanced manner as previously described (Xu et al., 2008; Xu et al., 2010). Food was given to individually housed mice thirty minutes after treatment.

Blood glucose, glucose, and insulin tolerance tests

For GTTs, chow-fed weight-matched animals were fasted for 18 hours (starting at 3 p.m.) with water provided *ad libitum*. At 9:00 a.m. of the next day, blood glucose levels were monitored at 15, 30, 60, 90, and 120 minutes after an i.p. dose of glucose (1.5 g/kg body weight). For ITTs, chow-fed weight-matched mice were fasted for 2 hours with water *ad libitum* on the experiment day. Mice were given an i.p. dose of insulin (1 U/kg, Eli Lilly and Company, HI-210), and blood glucose levels were monitored at 15, 30, 60, 90, and 120 minutes after insulin injection. Blood glucose was analyzed using an AlphaTrak (Abbott Laboratories, North Chicago, IL) meter designed for use in rodents.

Histology

Mice were anesthetized with an overdose of chloral hydrate (500mg/kg, i.p.) followed by transcardial perfusion with 10% formalin (in DEPC-treated saline). Brains were collected and then subjected to a two-hour postfix with 10% formalin (in DEPC-treated saline) before being cryoprotected in 30% sucrose (in 1XPBS) overnight at 4°C. On the next day, twenty-five μm coronal brain sections were prepared with a freezing microtome. The free-floating sections were stored in cryoprotectant at −20°C until needed for immunohistochemistry or RNA *in situ* hybridization. For immunostaining, sections were stained with primary antibodies against oxytocin (Cat# ab2078, abcam), arginine vasopressin (Cat# PA5-19819, Thermo Scientific), tyrosine hydroxylase (Cat# ab112, abcam), c-FOS (Cat# sc-52-G Santa Cruz Biotechnology), and GFP (Cat# A6455, Life Technologies) followed by secondary antibodies with Alexa Fluor® 488 (Life Technologies) or DAB chromogen (DAKO) according to manufacturers' protocols. *In situ* hybridization was performed as described previously (Vianna et al., 2012). Riboprobes were made from amplified PCR fragments with T7 and T3 promoters incorporated into the primer sequences so that the PCR product could be directly used as a template for the synthesis of the sense and antisense riboprobes.

Electrophysiology

Whole-cell patch-clamp recordings from *Htr2c* neurons were conducted as previously described (Sohn et al., 2011). Briefly, 3- to 5-week-old male or female mice were deeply anesthetized with i.p. injection of 7% chloral hydrate or isoflurane inhalations and transcardially perfused with a modified ice-cold artificial CSF (ACSF) (described below), in which an equiosmolar amount of sucrose was substituted for NaCl. The mice were then decapitated, and the entire brain was removed, and immediately submerged in ice-cold, carbogen-saturated (95% O_2 and 5% CO_2) ACSF (126 mM NaCl, 2.8 mM KCl, 1.2 mM $MgSO_4$, 2.5 mM $CaCl_2$, 1.25 mM NaH_2PO_4, 26 mM $NaHCO_3$, and 5 mM glucose). A brain block containing the hypothalamus was made. Coronal sections (250 μm) were cut with a Leica VT1000S or VT1200S Vibratome and then incubated in oxygenated ACSF at room temperature for at least 1 h before recording. Slices were transferred to the recording chamber and allowed to equilibrate for 10–20 min before recording. The slices were bathed in oxygenated ACSF (32°C–34°C) at a flow rate of ∼4 ml/min. The pipette solution for whole-cell recording was modified to include an intracellular dye (Alexa Fluor 488) for whole-cell recording: 120 mM K-gluconate, 10 mM KCl, 10 mM HEPES, 5 mM EGTA, 1 mM $CaCl_2$, 1 mM $MgCl_2$, and 2 mM MgATP, 0.03 mM Alexa Fluor 488 hydrazide dye, pH 7.3. Epifluorescence was briefly used to target fluorescent cells, at which time the light source was switched to infrared differential interference contrast imaging to obtain the whole-cell recording (Zeiss Axioskop FS2 Plus equipped with a fixed stage and a QuantEM:512SC electron-multiplying charge-coupled device camera or Nikon Eclipse FN1 equipped with a fixed stage and an optiMOS scientific CMOS camera). Electrophysiological signals were recorded using an Axopatch 700B amplifier (Molecular Devices), low-pass filtered at 2–5 kHz, and analyzed offline on a PC with pCLAMP programs (Molecular Devices). Recording electrodes had resistances of 2.5–5 MΩ when filled with the K-gluconate internal solution. Input resistance was assessed by measuring voltage deflection at the end of the response to a hyperpolarizing rectangular current pulse steps (500 ms of −10 to −50 pA or −5 to −25 pA). TTX, CNQX, AP5, picrotoxin, U73122, pertussis toxin, and 5-HT were obtained from Tocris. Anti-Gq antibody was obtained from Merck Millipore. Tolbutamide and glibenclamide were obtained from Sigma-Aldrich. All solutions were made according to the manufacturer's specifications. Stock solutions of U73122 were made by dissolution in DMSO (Sigma-Aldrich). The concentration of DMSO in the external solution was maintained below 0.1%. Stock solutions of tolbutamide were made by dissolution in 100% ethanol, with the final ethanol concentration in ACSF less than 0.5%. Stock solutions of all other drugs were made by dissolution in distilled water. Membrane potential values were not compensated to account for junction potential (−8 mV).

Stereotaxic injections

Detailed experimental procedures were carried out according to a published protocol (Cetin et al., 2006). Briefly, six to eight-week-old *Htr2c-Cre* mice were deeply anesthetized by an i.p. dose of ketamine/xylazine. Mice were placed into a stereotaxic frame and a small opening was made in the skull directly over the injection site (bregma, AP, −0.7mm, DV, −4.5mm, ± 0.2mm from bregma). Coordinates for stereotaxic injections were obtained from the Paxinos mouse brain atlas. About 75-100 nL of AAV viruses that contain

either stimulatory (hM3Dq) or inhibitory (hM4Di) DREADD constructs (AAV serotype 2 or 8, UNC viral core) were pressure injected into the PVH (unilateral or bilateral). After injection, all animals were allowed to recover for at least three weeks before being used for the feeding studies.

QUANTIFICATION AND STATISTICAL ANALYSIS

Replicate information is indicated in the figure legends. All results are given as mean ± SEM and analyzed by using statistical tools implemented in Prism (GraphPad version 9). Statistical analyses were performed using the Student's t test and regular one-way or two-way analysis of variance (ANOVA). Differences with $p < 0.05$ were considered to be significant. $p < 0.05$ (*), $p < 0.01$ (**), and $p < 0.001$ (***).